Phase-regenerative wavelength conversion in periodically poled lithium niobate waveguides

Sheng Liu,[1,*] Kwang Jo Lee,[1,3] Francesca Parmigiani,[1] Joseph Kakande,[1] Katia Gallo,[2] Periklis Petropoulos,[1] and David J. Richardson[1]

[1]*Optoelectronics Research Centre, University of Southampton, Southampton, SO17 1BJ, United Kingdom*
[2]*Department of Applied Physics, Royal Institute of Technology (KTH), 10691 Stockholm, Sweden*
[3]*Currently with Centre for Ultrahigh Bandwidth Devices for Optical Systems (CUDOS), School of Physics, University of Sydney, Sydney, New South Wales 2006, Australia*
** shl@orc.soton.ac.uk*

Abstract: We propose and experimentally demonstrate phase-regenerative wavelength conversion in periodically poled lithium niobate waveguides, using either: a single-stage implementation based on a simultaneous combination of two cascaded second-order nonlinear effects in a single periodically poled lithium niobate waveguide, or a two-stage implementation where two separate devices are used in sequence to give rise to the same nonlinear effects. The phase regeneration properties of the proposed wavelength conversion schemes are also investigated.

OCIS codes: (060.4510) Optical communications; (130.3730) Lithium niobate; (190.2620) Harmonic generation and mixing; (190.4410) Nonlinear optics, parametric processes; (190.4970) Parametric oscillators and amplifiers; (230.4320) Nonlinear optical devices.

References and links

1. C. J. McKinstrie, and S. Radic, "Phase-sensitive amplification in a fiber," Opt. Express **12**(20), 4973–4979 (2004).
2. R. Slavík, F. Parmigiani, J. Kakande, C. Lundstrom, M. Sjodin, P. Andrekson, R. Weerasuriya, S. Sygletos, A. Ellis, L. Grüner-Nielsen, D. Jakobsen, S. Herstrøm, R. Phelan, J. O'Gorman, A. Bogris, D. Syvridis, S. Dasgupta, P. Petropoulos, and D. J. Richardson, "All-optical phase and amplitude regenerator for next-generation telecommunications systems," Nat. Photonics **4**(10), 690–695 (2010).
3. K. Croussore, and G. Li, "Phase-regenerative DPSK wavelength conversion," in *Proceedings of IEEE Conference on Lasers and Electro-Optic Society (LEOS)* (Lake Bueta Vista, Florida, 2007), pp. 147–148.
4. K. Croussore, and G. Li, "Phase-regenerative wavelength conversion for BPSK and DPSK signals," IEEE Photon. Technol. Lett. **21**(2), 70–72 (2009).
5. M. Shirasaki, and H. A. Haus, "Squeezing of pulses in a nonlinear interferometer," J. Opt. Soc. Am. B **7**(1), 30–34 (1990).
6. M. E. Marhic, C. H. Hsia, and J. M. Jeong, "Optical amplification in a nonlinear fiber interferometer," Electron. Lett. **27**(3), 210–211 (1991).
7. K. J. Lee, F. Parmigiani, S. Liu, J. Kakande, P. Petropoulos, K. Gallo, and D. Richardson, "Phase sensitive amplification based on quadratic cascading in a periodically poled lithium niobate waveguide," Opt. Express **17**(22), 20393–20400 (2009).
8. C. Langrock, S. Kumar, J. E. McGeehan, A. E. Willner, and M. M. Fejer, "All-optical signal processing using $\chi^{(2)}$ nonlinearities in guided-wave devices," J. Lightwave Technol. **24**(7), 2579–2592 (2006).
9. K. Gallo, G. Assanto, and G. I. Stegeman, "Efficient wavelength shifting over the erbium amplifier bandwidth via cascaded second order processes in lithium niobate waveguides," Appl. Phys. Lett. **71**(8), 1020–1022 (1997).
10. M. H. Chou, I. Brener, M. M. Fejer, E. E. Chaban, and S. B. Christman, "1.5-μm-band wavelength conversion based on cascaded second-order nonlinearity in $LiNbO_3$ waveguides," IEEE Photon. Technol. Lett. **11**(6), 653–655 (1999).
11. J. Wang, J. Sun, X. Zhang, D. Huang, and M. M. Fejer, "All-optical format conversions using periodically poled lithium niobate waveguides," IEEE J. Quantum Electron. **45**(2), 195–205 (2009).
12. J. E. McGeehan, M. Giltrelli, and A. E. Willner, "All-optical digital 3-input AND gate using sum- and difference-frequency generation in a PPLN waveguide," Electron. Lett. **43**(7), 409–410 (2007).
13. Y. Wang, C. Yu, L. Yan, A. E. Willner, R. Roussev, C. Langrock, M. M. Fejer, J. E. Sharping, and A. L. Gaeta, "44-ns continuously tunable dispersionless optical delay element using a PPLN waveguide with two-pump configuration, DCF, and a dispersion compensator," IEEE Photon. Technol. Lett. **19**(11), 861–863 (2007).
14. S. Liu, K. J. Lee, K. Gallo, P. Petropoulos, and D. J. Richardson, "Elimination of the chirp of optical pulses through cascaded nonlinearities in periodically poled lithium niobate waveguides," Opt. Lett. **35**(22), 3724–3726 (2010).

#142977 - $15.00 USD Received 22 Feb 2011; revised 13 Apr 2011; accepted 14 Apr 2011; published 1 Jun 2011

15. S. Liu, K. J. Lee, F. Parmigiani, K. Gallo, P. Petropoulos, and D. J. Richardson, "Retiming of short pulses using quadratic cascading in a periodically poled lithium niobate waveguide," IEEE Photon. Technol. Lett. **23**(2), 94–96 (2011).
16. C. J. McKinstrie, and M. G. Raymer, "Four-wave-mixing cascades near the zero-dispersion frequency," Opt. Express **14**(21), 9600–9610 (2006).
17. C. J. McKinstrie, S. Radic, M. G. Raymer, and L. Schenato, "Unimpaired phase-sensitive amplification by vector four-wave mixing near the zero-dispersion frequency," Opt. Express **15**(5), 2178–2189 (2007).
18. T. Suhara, and M. Fujimura, *Waveguide Nonlinear-Optic Devices* (Springer, 2003), Chap. 11.
19. K. Gallo, and G. Assanto, "Analysis of lithium niobate all-optical wavelength shifters for the third spectral window," J. Opt. Soc. Am. B **16**(5), 741–753 (1999).
20. E. Ip, A. P. Lau, D. J. Barros, and J. M. Kahn, "Coherent detection in optical fiber systems," Opt. Express **16**(2), 753–791 (2008).
21. D. S. Hum, and M. M. Fejer, "Quasi-phasematching," C. R. Phys. **8**(2), 180–198 (2007).

1. Introduction

Phase-sensitive amplifiers (PSAs) have the potential to play a critical role in the regeneration of phase encoded signals. PSAs are capable of regenerating phase encoded signals by suppressing the cumulative linear phase noise added by the optical amplifiers and the nonlinear phase noise caused by nonlinear effects in fibres. Several PSA configurations have been demonstrated based on a number of technologies including: four-wave mixing (FWM) in highly nonlinear fibres (HNLF) [1–4], Kerr effects in nonlinear interferometers [5,6], and cascaded second-order nonlinearities in periodically poled lithium niobate (PPLN) waveguides [7]. A new kind of PSA based on FWM in a HNLF has recently been experimentally demonstrated which provides phase-regenerative wavelength conversion (PR-WC) [3,4]. In that configuration, two idlers at two new wavelengths are generated in a phase-sensitive fashion during a single stage of FWM interaction. Thereby, perfect phase regeneration of differential (bipolar) phase-shift keying (D(B)PSK) signals can in principle be achieved without necessarily requiring a large FWM conversion efficiency. Moreover, compared to other PSA implementations, wavelength conversion, an additional important network function, is performed at the same time. Hence PR-WC is of considerable interest for next generation meshed transparent networks.

In recent years, the use of cascaded second-order nonlinearities in PPLN waveguides has attracted much attention as a promising route to realizing all-optical signal processing functions [8]. Advantages of the technology include a high nonlinear coefficient (and consequently very compact devices), ultra-fast optical response, low cross talk, low spontaneous emission noise, no intrinsic frequency chirp, and transparency within bounds to bit rate. Cascaded second-harmonic and difference-frequency generation (cSHG/DFG) and cascaded sum- and difference-frequency generation (cSFG/DFG) have both been exploited in various all-optical signal processing applications such as: wavelength conversion [9,10], format conversion [11], logic gates [12], tunable optical time delay generation [13], chirp elimination [14], and pulse retiming [15].

Here, we report two different implementations of a novel scheme for PR-WC based on combinations of cSHG/DFG and cSFG/DFG in PPLN waveguides. The basic operational principle of our scheme can be intuitively represented in the complex plane of the E-field (i.e., the electric field of an optical wave is represented by a vector whose length represents the E-field amplitude and the angle represents the E-field phase), as shown in Fig. 1. The scheme operates by generating two phase-preserving copies of the incoming signal. One copy (generated through cSFG/DFG) is an exact replica of the input, whereas the other (generated through cSHG/DFG) is its phase conjugate. These two outputs are equalized in power and combined. In the complex plane of the E-field, the combined output is aligned to the in-phase axis. Therefore, a noisy input D(B)PSK signal is phase-regenerated to produce an output signal which in principle has an exact phase value of either 0 or π. PR-WC exploiting cascaded second-order nonlinearities in PPLN waveguides offers a number of advantages over the corresponding FWM-based fibre approach. Firstly, PPLN waveguides are compact and effectively immune to stimulated Brillouin scattering of the pump beams. Furthermore, in contrast to fibre-based implementations PR-WC exploiting cascaded second-order

#142977 - $15.00 USD Received 22 Feb 2011; revised 13 Apr 2011; accepted 14 Apr 2011; published 1 Jun 2011

nonlinearities in PPLN waveguides is far less susceptible to the generation of pump-pump and pump-signal harmonics [16,17], as well as to self-phase and cross-phase modulation [3].

In the following, we present experimental demonstrations of this scheme, employing either two separate PPLN waveguides for the implementation of the cSFG/DFG and cSHG/DFG processes, or just a single waveguide in which the nonlinear processes develop simultaneously. The paper is organized as follows. An analytical presentation of the two schemes is given in Section 2; we have chosen to describe the two-stage PR-WC implementation first (Section 2.1) because the analysis is simpler. The presentation of the single-stage PR-WC implementation follows in Section 2.2. Our experimental demonstrations are presented in Section 3. Due to the relatively simpler experimental setup, the single-stage PR-WC experiments are described first (Section 3.1) followed by the two-stage PR-WC experiments (Section 3.2) which include direct phase regeneration measurements. The paper is summarized in Section 4.

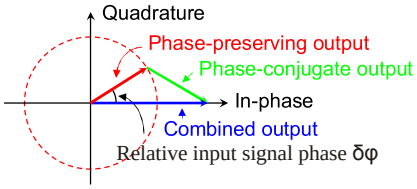

Fig. 1. Operational principle of the phase-regenerative wavelength conversion.

2. Theory

2.1 Two-stage implementation

Figure 2 illustrates the wavelength arrangement for the two-stage PR-WC implementation based on a combination of cascaded second-order nonlinearities in two separate PPLN waveguides (i.e. cSFG/DFG in the first PPLN and cSHG/DFG in the second PPLN).

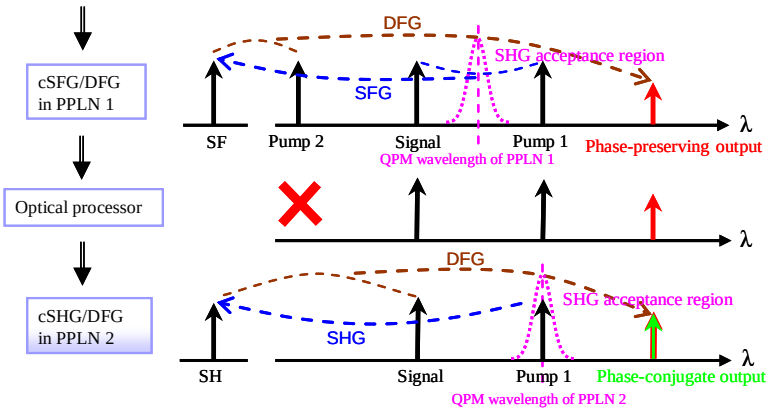

Fig. 2. Illustration of two-stage phase-regenerative wavelength conversion based on cSFG/DFG and cSHG/DFG in two separate PPLN waveguides.

The quasi-phase-matching (QPM) wavelengths of the first (PPLN 1) and the second PPLN waveguides (PPLN 2) are detuned relative to each other, and arranged so that Pump 1 and the input signal are placed symmetrically around the QPM wavelength of PPLN 1. Also the wavelength of Pump 1 coincides with the QPM wavelength of PPLN 2. Pump 2 is set at a frequency such that Pump 2, Signal, and Pump 1 have the same frequency spacing between them. The input Signal, Pump 1, and Pump 2 are phase-locked relative to each other and launched into PPLN 1. As shown in Fig. 2, the input Signal and Pump 1 generate the sum frequency (SF) wave by SFG in PPLN 1, followed by the DFG process between the SF wave and Pump 2, which generates the phase-preserving output at a new wavelength. The evolution

#142977 - $15.00 USD Received 22 Feb 2011; revised 13 Apr 2011; accepted 14 Apr 2011; published 1 Jun 2011

of the interacting waves associated with the cSFG/DFG process in PPLN 1 can be described through the following set of coupled mode equations [18]:

$$\begin{aligned}
\frac{dA_{p1}}{dz} &= i\omega_{p1}\kappa_{SFG}A_{sf}A_s^*\exp(i\Delta k_{SFG}z),\\
\frac{dA_s}{dz} &= i\omega_s\kappa_{SFG}A_{sf}A_{p1}^*\exp(i\Delta k_{SFG}z),\\
\frac{dA_{sf}}{dz} &= i\omega_{sf}\kappa_{SFG}A_sA_{p1}\exp(-i\Delta k_{SFG}z)+i\omega_{sf}\kappa_{DFG}A_{p2}A_{out}\exp(-i\Delta k_{DFG}z),\\
\frac{dA_{p2}}{dz} &= i\omega_{p2}\kappa_{DFG}A_{sf}A_{out}^*\exp(i\Delta k_{DFG}z),\\
\frac{dA_{out}}{dz} &= i\omega_{out}\kappa_{DFG}A_{sf}A_{p2}^*\exp(i\Delta k_{DFG}z),
\end{aligned} \tag{1}$$

where A_j (j = $p1$, $p2$, sf, s, out) are the complex amplitudes of Pump 1, Pump 2, the SF, Signal and the output respectively, ω_j are the angular frequencies, κ_{SFG} and κ_{DFG} are the nonlinear coupling coefficients of the SFG process and the DFG process respectively, and Δk_{SFG} and Δk_{DFG} are the phase mismatches of the SFG process and the DFG process respectively. Δk_{SFG} = 0 since Pump 1 and the Signal are placed symmetrically around the QPM wavelength. Δk_{DFG} is also close to zero because of the low dispersion of lithium niobate crystals in the wavelength region around 1550 nm. Note that for simplicity the waveguide loss has not been taken into account in Eq. (1). By integrating the coupled-mode equations for cSFG/DFG under the non-depletion approximation, the complex amplitude of the cSFG/DFG output can be approximated as:

$$\begin{aligned}
A_{cSFG/DFG} &\approx \frac{1}{2}\omega_{out}\omega_{sf}\kappa_{SFG}\kappa_{DFG}A_{p1}A_sA_{p2}^*L^2\\
&= \frac{1}{2}\omega_{out}\omega_{sf}\kappa_{SFG}\kappa_{DFG}\left|A_{p1}\right|\left|A_s\right|\left|A_{p2}\right|L^2e^{i(\varphi_{p1}-\varphi_{p2}+\varphi_s)}\\
&= \frac{1}{2}\omega_{out}\omega_{sf}\kappa_{SFG}\kappa_{DFG}\left|A_{p1}\right|\left|A_s\right|\left|A_{p2}\right|L^2e^{i(\frac{3}{2}\varphi_{p1}-\frac{1}{2}\varphi_{p2}+\delta\varphi)},
\end{aligned} \tag{2}$$

where L is the length of PPLN 1. φ_{p1}, φ_{p2}, and φ_s also denote the phases of Pump 1, Pump 2, and Signal respectively. The relative input signal phase, $\delta\varphi$, is defined as $(\delta\varphi_1 + \delta\varphi_2)/2$, where $\delta\varphi_1 = \varphi_s - \varphi_{p1}$ is the relative phase between Signal and Pump 1, and $\delta\varphi_2 = \varphi_s - \varphi_{p2}$ is the relative phase between Signal and Pump 2.

Pump 2 is suppressed after PPLN 1, and the rest of the optical waves are subsequently launched into PPLN 2. In the cSHG/DFG process occurring within PPLN 2, the second harmonic (SH) wave of Pump 1 is generated by the SHG process, and this is accompanied by the DFG process between the SH wave and the input Signal which produces its phase-conjugate output. The evolution of the interacting waves associated with the cSHG/DFG process in PPLN 2 can be described through the following set of coupled mode equations [19]:

#142977 - $15.00 USD Received 22 Feb 2011; revised 13 Apr 2011; accepted 14 Apr 2011; published 1 Jun 2011

$$
\begin{aligned}
\frac{dA_{p1}}{dz} &= i\omega_{p1}\kappa_{SHG}A_{sh}A_{p1}^{*}\exp(i\Delta k_{SHG}z),\\
\frac{dA_{sh}}{dz} &= \frac{i}{2}\omega_{sh}\kappa_{SHG}A_{p1}^{2}\exp(-i\Delta k_{SHG}z)+i\omega_{sh}\kappa_{DFG}A_{s}A_{out}\exp(-i\Delta k_{DFG}z),\\
\frac{dA_{s}}{dz} &= i\omega_{s}\kappa_{DFG}A_{sh}A_{out}^{*}\exp(i\Delta k_{DFG}z),\\
\frac{dA_{out}}{dz} &= i\omega_{out}\kappa_{DFG}A_{sh}A_{s}^{*}\exp(i\Delta k_{DFG}z),
\end{aligned}
\tag{3}
$$

where A_j (the subscript j = $p1$, sh, s, out) are the complex amplitudes of Pump 1, the SH, Signal and the output respectively, κ_{SHG} is the nonlinear coupling coefficient of the SHG process, and Δk_{SHG} is the phase mismatch of the SHG process. Note that $\Delta k_{SHG} = 0$ as Pump 1 is set at the SHG QPM wavelength, whereas as before, $\Delta k_{DFG} \approx 0$. Under the non-depletion approximation and by integrating the coupled-mode equations for cSHG/DFG, the complex amplitude of the cSHG/DFG output can be approximated as:

$$
\begin{aligned}
\mathrm{A}_{cSHG/DFG} &\approx \frac{1}{4}\omega_{out}\omega_{sh}\kappa_{SHG}\kappa_{DFG}{A_{p1}}^{2}A_{s}^{*}L^{2}\\
&= \frac{1}{4}\omega_{out}\omega_{sh}\kappa_{SHG}\kappa_{DFG}\left|A_{p1}\right|^{2}\left|A_{s}\right|L^{2}e^{i(\frac{3}{2}\varphi_{p1}-\frac{1}{2}\varphi_{p2}-\delta\varphi)},
\end{aligned}
\tag{4}
$$

where L is the length of PPLN 2.

Since Pump 2, Signal, and Pump 1 have the same frequency spacing between them, the outputs from cSHG/DFG and cSFG/DFG are generated at the same wavelength. Thus these two outputs are combined. If for simplicity, we assume that the two waveguides have the same length, and the intensities of the two outputs are equalised by adjusting the power of Pump 2, then the complex amplitude of the combined output can be approximated as:

$$
\begin{aligned}
\mathrm{A} &\approx \frac{1}{2}\omega_{out}\omega_{sf}\kappa_{SFG}\kappa_{DFG}\left|A_{p1}\right|\left|A_{s}\right|\left|A_{p2}\right|L^{2}e^{i(\frac{3}{2}\varphi_{p1}-\frac{1}{2}\varphi_{p2}+\delta\varphi)}\\
&+\frac{1}{4}\omega_{out}\omega_{sh}\kappa_{SHG}\kappa_{DFG}\left|A_{p1}\right|^{2}\left|A_{s}\right|L^{2}e^{i(\frac{3}{2}\varphi_{p1}-\frac{1}{2}\varphi_{p2}-\delta\varphi)}\\
&= \omega_{out}\omega_{sf}\kappa_{SFG}\kappa_{DFG}\left|A_{p1}\right|\left|A_{p2}\right|\left|A_{s}\right|L^{2}e^{i(\frac{3}{2}\varphi_{p1}-\frac{1}{2}\varphi_{p2})}\cos(\delta\varphi).
\end{aligned}
\tag{5}
$$

In the ideal case, the combination of the phase-conjugate output from cSHG/DFG and the phase-preserving output from cSFG/DFG results in perfect cancellation of the quadrature component of the output and amplification of the in-phase component, as shown in Eq. (5). It is noted that this regenerative property is independent of the conversion efficiency of the cSHG/DFG and the cSFG/DFG processes.

2.2 Single-stage implementation

The two separate nonlinear stages described above can also be combined within a single PPLN waveguide, thereby benefitting from an implementation that requires fewer components. Figure 3 illustrates the wavelength arrangement for the proposed single-stage PR-WC implementation based on the simultaneous combination of the cSHG/DFG and cSFG/DFG processes in a single PPLN waveguide. The input Signal, Pump 1, and Pump 2 are phase-locked relative to each other and launched into the PPLN waveguide. In order to allow the two cascaded processes to occur simultaneously in the same device they need to be detuned from the exact phase-matching conditions. As shown in Fig. 3, it is necessary to ensure that Pump 1 still falls within the SHG acceptance bandwidth and that the mean wavelength of the input Signal and Pump 1 also falls within it. In addition, Pump 2 needs to

#142977 - $15.00 USD Received 22 Feb 2011; revised 13 Apr 2011; accepted 14 Apr 2011; published 1 Jun 2011

be set at a frequency which equalises the frequency difference between Pump 2 and Signal, and Signal and Pump 1.

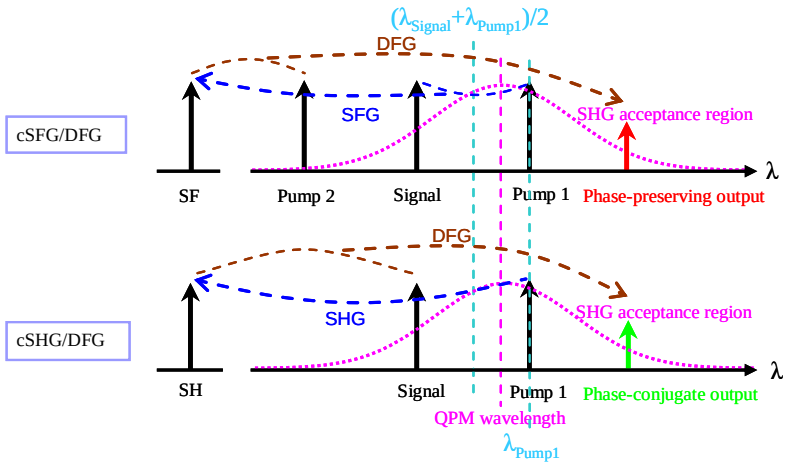

Fig. 3. Illustration of single-stage phase-regenerative wavelength conversion based on cSFG/DFG and cSHG/DFG in a single PPLN waveguide.

The input Signal and Pump 1 generate the SF wave by the SFG process. When followed by DFG between the SF wave and Pump 2 a phase-preserving output at a new wavelength [see Fig. 3(a)] is generated. At the same time, the SH wave of Pump 1 is generated in the PPLN waveguide as shown in Fig. 3(b), and this is accompanied by DFG between this SH wave and the input signal to produce its phase-conjugate output at a new wavelength. Since Pump 2, Signal and Pump 1 are arranged to have the same frequency spacing between them, the outputs from cSHG/DFG and cSFG/DFG are therefore generated at the same wavelength. If for simplicity, we assume that the phase mismatches of the SHG and the SFG process are equal but with opposite sign and nonzero ($\Delta k_{SHG} = -\Delta k_{SFG} \neq 0$) due to the detuning of both cSHG/DFG and cSFG/DFG from the exact phase-matching conditions (which is in contrast to the aforementioned two-stage implementation), then the coupled-mode equations for cSFG/DFG under the non-depletion approximation can be integrated and the complex amplitude of the cSFG/DFG output can be approximated as:

$$\begin{aligned} A_{cSFG/DFG} &\approx -\frac{\kappa_{DFG}\omega_{output}\kappa_{SFG}\omega_{sf}A_{p1}A_s A_{p2}^*}{\Delta k_{SFG}}\int_0^L (e^{-i\Delta k_{SFG}z}-1)\,e^{i\Delta k_{DFG}z}\,dz \\ &\approx \kappa_{DFG}\omega_{out}\kappa_{SFG}\omega_{sf}\left|A_{p1}\right|\left|A_s\right|\left|A_{p2}\right|L^2\mathrm{sinc}(\Delta k_{SFG}L/2)e^{i(\frac{3}{2}\varphi_{p1}-\frac{1}{2}\varphi_{p2})}e^{i\delta\varphi+i\Delta k_{SFG}L/4}, \end{aligned} \tag{6}$$

where $\Delta k_{DFG} \approx 0$, because of the low dispersion feature of lithium niobate crystals in the wavelength region around 1550 nm, and $\mathrm{sinc}(x) = \sin(x)/x$. By integrating the coupled-mode equations for cSHG/DFG under the non-depletion approximation, the complex amplitude of the cSHG/DFG output can be approximated as:

$$\begin{aligned} A_{cSHG/DFG} &\approx \frac{1}{2}\frac{\kappa_{DFG}\omega_{out}\kappa_{SHG}\omega_{sh}A_{p1}^2A_s^*}{\Delta k_{SHG}}\int_0^L (e^{-i\Delta k_{SHG}z}-1)\,e^{i\Delta k_{DFG}z}\,dz \\ &\approx \frac{1}{2}\kappa_{DFG}\omega_{out}\kappa_{SHG}\omega_{sh}\left|A_{p1}\right|^2\left|A_s\right|L^2\mathrm{sinc}(\Delta k_{SHG}L/2)e^{i(\frac{3}{2}\varphi_{p1}-\frac{1}{2}\varphi_{p2})}e^{-i\delta\varphi+i\Delta k_{SHG}L/4}, \end{aligned} \tag{7}$$

#142977 - $15.00 USD Received 22 Feb 2011; revised 13 Apr 2011; accepted 14 Apr 2011; published 1 Jun 2011

where $\Delta k_{DFG} \approx 0$ as before. We also assume that the intensities of the two outputs are equalized by adjusting the power of Pump 2, in which instance the complex amplitude of the combined output can be approximated as:

$$\begin{aligned} A &\approx \frac{1}{2}\omega_{out}\omega_{sf}\kappa_{SFG}\kappa_{DFG}\left|A_{p1}\right|\left|A_{p2}\right|\left|A_s\right|L^2\mathrm{sinc}(\Delta k_{SFG}L/2)e^{i(\frac{3}{2}\varphi_{p1}-\frac{1}{2}\varphi_{p2})}e^{i\delta\varphi+i\Delta k_{SFG}L/4} \\ &+\frac{1}{4}\omega_{out}\omega_{sh}\kappa_{SHG}\kappa_{DFG}\left|A_{p1}\right|^2\left|A_s\right|L^2\mathrm{sinc}(\Delta k_{SHG}L/2)e^{i(\frac{3}{2}\varphi_{p1}-\frac{1}{2}\varphi_{p2})}e^{-i\delta\varphi+i\Delta k_{SHG}L/4} \\ &=\omega_{out}\omega_{sf}\kappa_{SFG}\kappa_{DFG}\left|A_{p1}\right|\left|A_{p2}\right|\left|A_s\right|L^2\mathrm{sinc}(\Delta k_{SFG}L/2)e^{i(\frac{3}{2}\varphi_{p1}-\frac{1}{2}\varphi_{p2})}\cos(\delta\varphi'), \end{aligned} \quad (8)$$

where A_j (j = $p1$, $p2$, s) denote the complex amplitudes of Pump 1, Pump 2 and the Signal respectively. $\delta\varphi' = \delta\varphi + \Delta k_{SFG}L/4$ is the summation of the relative input phase plus the phase shift induced by the nonzero phase-mismatches of the SHG and the SFG processes.

Compared to the two-stage scheme, the conversion efficiency of the cSHG/DFG process and the cSFG/DFG process in the single-stage scheme is compromised by the nonzero phase-mismatches resulting in a lower output power. However, in principle, the combination of the phase-conjugate output and the phase preserving output still results in amplification of the in-phase component of the signal and cancellation of the quadrature component, as shown in Eq. (8). This regenerative property is independent of the conversion efficiency of the cSHG/DFG and the cSFG/DFG processes. A limitation of the single-stage implementation is that the operational bit rate of the input signal (i.e. the signal bandwidth) is restricted by the frequency spacing between the signal and the pumps which in turn, is limited by the SHG acceptance bandwidth of the PPLN waveguide.

In the following section, we present two separate experiments that have demonstrated the PR-WC proposed above in either a single- or a two-stage implementation, employing either one or two nominally identical PPLN devices as the nonlinear media respectively. The implementation of the single-stage PR-WC is simpler and is presented first. Fuller measurements of the phase-correction performance of the scheme are presented for the more flexible two-stage implementation that follows in Section 3.2.

3. Experiments

3.1 Single-stage implementation

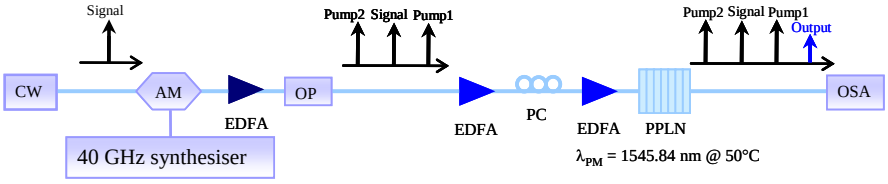

Fig. 4. Experimental setup for the proposed single-stage PR-WC based on a combination of cSHG/DFG and cSFG/DFG. AM: amplitude modulator, PC: polarization controller, EDFA: erbium-doped fibre amplifier, OSA: optical spectrum analyser, OP: optical processor.

Figure 4 shows the experimental setup used to realize the single-stage PR-WC. A 30-mm-long fibre-pigtailed PPLN waveguide (HC Photonics Corp.) was used to observe both cSHG/DFG and cSFG/DFG in a single stage. Its SHG phase matching wavelength was ~1545.84 nm at 50°C, its insertion loss was 3.5 dB and its normalised (internal) conversion efficiency was 75%$W^{-1}cm^{-2}$. A continuous wave (CW) laser operating at 1545.68 nm was modulated by an amplitude modulator driven by a 40 GHz synthesiser, generating three frequency tones at 1545.36 nm, 1545.68 nm and 1546.00 nm respectively. These three tones were used as Pump 2, the input Signal, and Pump 1, respectively. All of the frequency tones were subsequently passed through an optical processor (Finisar Waveshaper 4000E), which is

#142977 - $15.00 USD Received 22 Feb 2011; revised 13 Apr 2011; accepted 14 Apr 2011; published 1 Jun 2011

a programmable filter used to adjust both the relative phase between the three waves and the optical power of Pump 2, thereby controlling the strength of the cSFG/DFG process in the PPLN waveguide. All of the optical waves were aligned to the optical axis of the PPLN waveguide by a polarisation controller, amplified (to a total power of 21 dBm) and subsequently launched into the PPLN waveguide. Both the phase-preserving output of the cSFG/DFG process and the phase-conjugate output of the cSHG/DFG process respectively lie at 1546.32 nm.

Figure 5(a) shows the measured spectra at the output of the PPLN waveguide for the cases of maximum (red trace) and minimum conversion efficiency (blue trace) at the combined output. Note that these measurements were achieved by controlling the relative phase of the signal at 1545.68 nm in the OP. The wavelength conversion loss for the case of maximum conversion was ~19.5 dB. We define the phase-sensitive swing (PSS) as the ratio between the maximum and minimum output power of the converted signal. The PSS of the combined output was ~14.5dB. From Eq. (8) we find that this corresponds to an amplitude ratio of the cSHG/DFG and cSFG/DFG outputs of ~0.7:1. In contrast to the experimental results in Ref [7], the large PSS of the combined output is due to the strong attenuation of the quadrature component of the signal rather than the amplification of the in-phase component. Figure 5(b) shows the phase-sensitive behaviour of the combined output plotted as a function of the relative phase between the input signal and the pumps. The experimental measurements (red spots) agree well with the theoretical curve calculated using Eq. (8) (blue curve). The swing profile clearly indicates the phase-sensitive behaviour with a period of π-phase. Figure 5(b) also illustrates the calculated phase regenerative properties of the proposed single-stage PR-WC scheme. The black trace shows the ideal case, where the outputs from cSHG/DFG and cSFG/DFG are perfectly conjugated and have strictly equal powers. The cancellation of the quadrature component of the signal allows close to ideal binary phase regeneration, independent of the overall cSHG/DFG and cSFG/DFG efficiency. The red trace shows the calculated phase regenerative properties of the single-stage PR-WC scheme for a PSS of 14.5 dB as achieved in the experiment.

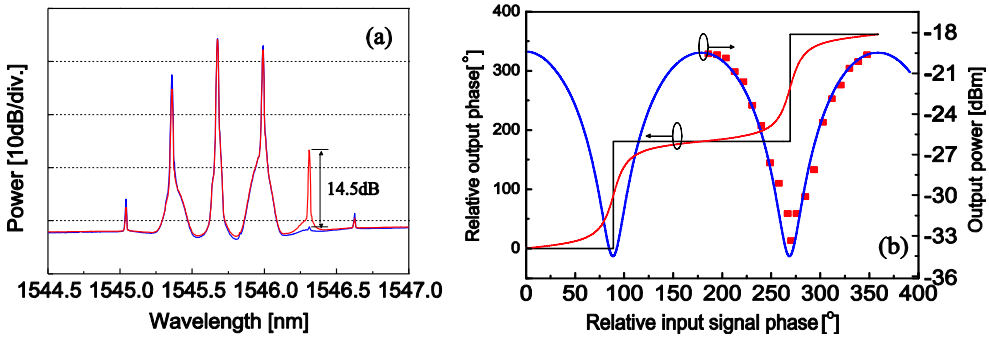

Fig. 5. (a) Measured output spectra of the single-stage PR-WC showing the phase-sensitive swing (measured with a resolution of 0.05 nm). (b) Measured (symbols) and calculated phase-sensitive swing (solid line) plotted as a function of the relative input signal phase for the single-stage PR-WC.

3.2 Two-stage implementation

Figure 6 shows the experimental setup used to realise the two-stage PR-WC with two cascaded PPLN waveguides. Both of the PPLN waveguides (HC Photonics Corp.) were nominally identical with parameters as shown in Section 3.1. The SHG QPM of PPLN 2 was shifted to 1548 nm by operating it at the higher temperature of 60°C. Two CW lasers were used as the signal source and Pump 1, operating at 1544nm and 1548 nm respectively. The two beams were combined in a 3-dB coupler, amplified and launched into 500 m of a HNLF to generate a phase-correlated idler wave at 1540 nm through FWM which was then used as Pump 2. The HNLF had a dispersion of −0.87 ps/nm·km at 1550 nm and a nonlinear

#142977 - $15.00 USD Received 22 Feb 2011; revised 13 Apr 2011; accepted 14 Apr 2011; published 1 Jun 2011

coefficient of 19 $(W \cdot km)^{-1}$. All of the optical waves were passed through Optical Processor 1 (OP1), which, as before, was used to adjust the relative phase between the signal and the pumps and to adjust the optical power of Pump 2, thereby controlling the strength of the cSFG/DFG process in PPLN1. After OP1, all of the optical waves were amplified (to a total power of 21 dBm) and launched into PPLN 1 which induced the cSFG/DFG process to generate the phase-preserving output at 1552 nm. All of the resulting optical waves were subsequently passed through a second optical processor (OP2), which selectively suppressed Pump 2. After OP2, all of the optical waves were amplified (to a total power of 21 dBm) and launched into PPLN 2 which induced the cSHG/DFG process to generate the phase-conjugate output, also at 1552 nm.

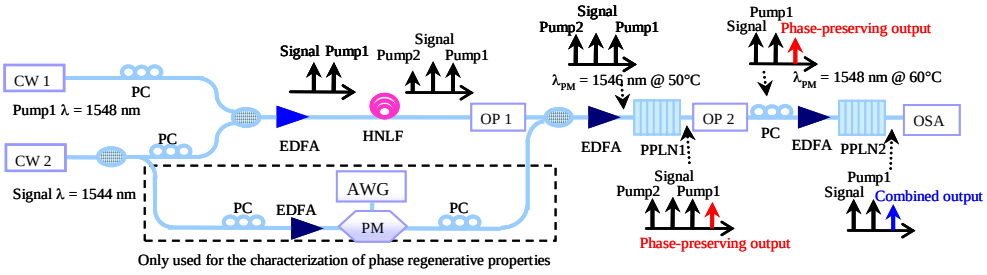

Fig. 6. Experimental setup for the two-stage PR-WC scheme based on a combination of cSHG/DFG and cSFG/DFG in two cascaded PPLN waveguides. CW: continuous wave, PC: polarization controller, EDFA: erbium-doped fibre amplifier, HNLF: highly nonlinear fibre, OP: optical processor, OSA: optical spectrum analyzer, PM: phase modulator, AWG: arbitrary waveform generator.

Figure 7(a) shows the measured spectra at the output of PPLN 2 for the cases of maximum (red trace) and minimum conversion efficiency (blue trace) at the combined output. Note that these measurements were achieved by controlling the relative phase of the signal at 1544 nm in OP1. The wavelength conversion loss for the case of maximum conversion was ~18 dB. The PSS of the combined output was ~25.3 dB. From Eq. (5) we find that this corresponds to an amplitude ratio of the cSHG/DFG and cSFG/DFG outputs of ~0.91:1.

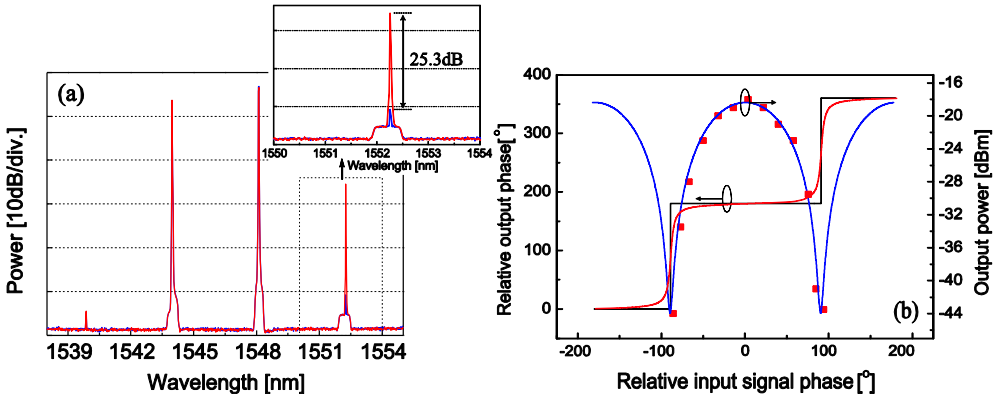

Fig. 7. (a) Measured output spectra of the two-stage PR-WC scheme showing the phase-sensitive swing (measured with a resolution of 0.05 nm). (b) The measured (red spots) and calculated phase-sensitive swing (blue curve) plotted as a function of the relative input signal phase, and the calculated input-output phase relationship of ideal case (black trace) and the two-stage PR-WC scheme (red trace).

Figure 7(b) shows the phase-sensitive behaviour of the combined output plotted as a function of the relative phase between the input signal and the pumps. The experimental measurements (red spots) agree well with the theoretical curve (blue curve). The swing profile

#142977 - $15.00 USD Received 22 Feb 2011; revised 13 Apr 2011; accepted 14 Apr 2011; published 1 Jun 2011

clearly indicates the phase-sensitive behaviour with a period of π-phase. Figure 7(b) also illustrates the calculated phase regenerative properties of the proposed two-stage PR-WC scheme. The black trace shows the ideal case, where the outputs from cSHG/DFG and cSFG/DFG are perfectly conjugated and have strictly equal powers. The red trace shows the calculated phase regenerative properties of the two-stage PR-WC scheme for a PSS of 25.3 dB as achieved in the experiment. Phase noise ranging between ± 30° at an input D(B)PSK signal can be suppressed to ~ ± 1.5° at the output. As with all basic PSA configurations, phase regeneration in our PS-WC scheme is achieved at the expense of some added amplitude noise. In our PR-WC scheme, a phase fluctuation of ± 30° is converted into an amplitude fluctuation of 0.62 dB. (This amplitude noise can be reduced e.g. by increasing the conversion efficiency of the PPLN waveguides and saturating the gain of the outputs.)

To characterize the phase regenerative capabilities of the system, the signal was split into two arms as illustrated in the dashed box shown in Fig. 6. The input Signal in the top arm was suppressed by OP1 after FWM, and a phase modulator was first used to emulate phase noise degradation of a binary phase modulated signal in the bottom arm. The modulator was driven by an electrical signal comprising the sum of a binary (signal) at 4 Gbit/s, and a broadband random noise waveform, generated using a 24 GS/s arbitrary waveform generator (Tektronix AWG7122B). To measure the phase characteristics, the input signal and the idler were assessed using a homodyne coherent receiver (see e.g. Ref [20]). Because the homodyne receiver requires a local oscillator at the original signal wavelength, the output was first converted back to the original signal wavelength using a parametric fibre wavelength converter using the output and Pump 1. The phase information was retrieved using digital signal processing, and the results are displayed in Fig. 8. The data were sampled at the sampling rate of 48 GHz, and one in every 12 samples was recorded in the digit signal processing (i.e. one recorded sample per bit). We show phase histograms (20000 recorded samples) of the input signal [Fig. 8(a)] and the (converted) output [Fig. 8(b)]. The input signal phase at the 0° peak is distributed with a 3dB width of ± 30°, while at the output the phase fluctuations have been considerably reduced, with a 3 dB distribution width of <10°. We attribute the difference between the experimental and calculated performance based on the response function shown in Fig. 7 to be due to relative phase drift/noise between the pump and signal arms induced by environmental perturbations. Such effects mean that it is not possible to guarantee that the PR-WC was operating at its optimal operating point during the measurement (i.e. inputs with 0^o relative phase experiencing the maximum gain). To make more reliable measurements (and most certainly for any practical application) it would be necessary to ensure that the signal and pump beams were accurately phase-locked – for example using an active phase lock loop (see, e.g., Ref [2]). The final 500 m-long fibre-based wavelength conversion stage, which we required to allow us to implement the homodyne coherent receiver, also presents an additional potential source of measurement noise. Nevertheless, these proof-of-principle measurements demonstrate significant phase noise reduction and validate the approach.

#142977 - $15.00 USD Received 22 Feb 2011; revised 13 Apr 2011; accepted 14 Apr 2011; published 1 Jun 2011

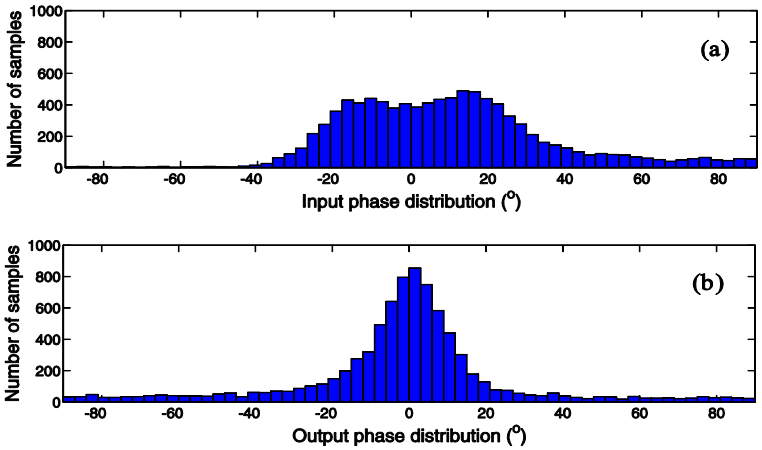

Fig. 8. (a) Measured phase distribution at the input and (b) the output.

4. Conclusion

We have demonstrated both theoretically and experimentally a novel scheme for PR-WC based on a combination of cSHG/DFG and cSFG/DFG processes. This scheme can be implemented in either a single PPLN waveguide, or two separate PPLN waveguides. We demonstrated a single-stage PR-WC using a single PPLN waveguide with a uniform poling period. A PSS of 14.5 dB was achieved in this experiment. In order to achieve the best regenerative performance both cSHG/DFG and cSFG/DFG need to be detuned from the exact phase-matching conditions and the maximum permissible signal bandwidth is restricted by the requirement to fit both the signal and one of the pumps within the SHG bandwidth of the PPLN device. These limitations could in principle be overcome by employing a superstructured PPLN waveguide exhibiting two QPM peaks [21]. In this case, both cSFG/DFG and cSHG/DFG could operate at the exact phase-matching conditions by placing Pump 1 and the input signal symmetrically around the first QPM wavelength of the PPLN waveguide, as well as placing Pump 1 at the second QPM wavelength of the PPLN waveguide.

The limitations imposed by the single-stage implementation were overcome by separating the two cascaded quadratic operations in two different PPLN waveguides. By doing this, a PSS of 25.3 dB was achieved. We verified the very good agreement between our theoretical predictions and the performance of our PR-WC scheme. The phase-regenerative properties of the wavelength converter were also verified using a purpose-built homodyne detection system. Our proof-of-principle experiments of the phase regenerative properties show the potential of our PR-WC scheme as a D(B)PSK phase regenerator.

Acknowledgement

The research leading to these results has received funding from the UK EPSRC under grant agreement EP/F032218/1. Katia Gallo gratefully acknowledges support from the EU under grant agreement PIEF-GA-2009-234798.

#142977 - $15.00 USD Received 22 Feb 2011; revised 13 Apr 2011; accepted 14 Apr 2011; published 1 Jun 2011